ACS APPLIED MATERIALS & INTERFACES

Research Article

www.acsami.org

Synergetic Approach for Simple and Rapid Conjugation of Gold Nanoparticles with Oligonucleotides

Jiuxing Li, Binqing Zhu, Xiujie Yao, Yicong Zhang, Zhi Zhu, Song Tu, Shasha Jia, Rudi Liu, Huaizhi Kang,* and Chaoyong James Yang*

The MOE Key Laboratory of Spectrochemical Analysis & Instrumentation, Collaborative Innovation Center of Chemistry for Energy Materials, the Key Laboratory of Chemical Biology of Fujian Province, State Key Laboratory of Physical Chemistry of Solid Surfaces, College of Chemistry and Chemical Engineering, Xiamen University, Xiamen 361005, China

Supporting Information

ABSTRACT: Attaching thiolated DNA on gold nanoparticles (AuNPs) has been extremely important in nanobiotechnology because DNA−AuNPs combine the programmability and molecular recognition properties of the biopolymers with the optical, thermal, and catalytic properties of the inorganic nanomaterials. However, current standard protocols to attach thiolated DNA on AuNPs involve time-consuming, tedious steps and do not perform well for large AuNPs, thereby greatly restricting applications of DNA−AuNPs. Here we demonstrate a rapid and facile strategy to attach thiolated DNA on AuNPs based on the excellent stabilization effect of mPEG-SH on AuNPs. AuNPs are first protected by mPEG-SH in the presence of Tween 20, which results in excellent stability of AuNPs in high ionic strength environments and extreme pHs. A high concentration of NaCl can be applied to the mixture of DNA and AuNP directly, allowing highly efficient DNA attachment to the AuNP surface by minimizing electrostatic repulsion. The entire DNA loading process can be completed in 1.5 h with only a few simple steps. DNA-loaded AuNPs are stable for more than 2 weeks at room temperature, and they can precisely hybridize with the complementary sequence, which was applied to prepare core−satellite nanostructures. Moreover, cytotoxicity assay confirmed that the DNA−AuNPs synthesized by this method exhibit lower cytotoxicity than those prepared by current standard methods. The proposed method provides a new way to stabilize AuNPs for rapid and facile loading thiolated DNA on AuNPs and will find wide applications in many areas requiring DNA−AuNPs, including diagnosis, therapy, and imaging.

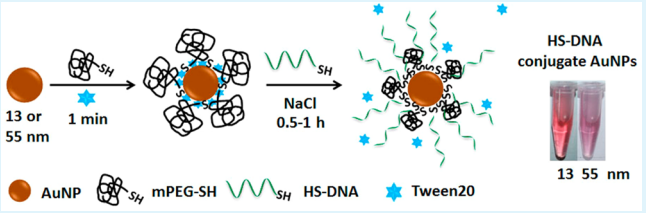

KEYWORDS: *Gold nanoparticle, DNA conjugation, bioconjugation, surface modification, self-assembly, surfactants*

INTRODUCTION

Gold nanoparticles (AuNPs) have become an integral part of research in nanoscience due to their excellent physical and chemical properties, such as extremely high extinction coefficients,[1] outstanding fluorescence quenching ability,[2−5] high chemical stability,[6,7] and significant catalytic ability.[8] Since 1996,[5] attachment of thiolated DNA has expanded the applications of AuNPs in areas such as preparation of crystal nanoparticle structures,[9−11] bioanalysis,[12,13] diagnostics,[14−17] therapeutics,[18−20] in vivo imaging,[18,21−23] intracellular RNA quantification,[24−26] and gene regulation.[27−30] The merits of DNA−AuNPs include (i) high stability because the negatively charged DNA acts as a charge and steric stabilizer in high ionic strength solutions,[31] (ii) excellent recognition capability due to Watson−Crick base pairing,[21,26,32,33] and (iii) capability of coupling to other molecules for drug delivery or molecular imaging.[26,34−36]

Despite these advantages, the long-standing challenges associated with attaching thiolated DNA on AuNPs still remain, greatly restricting application in many fields. In current standard protocols to attach thiolated DNA on AuNPs, a high concentration of NaCl is needed to screen the electrostatic repulsion and facilitate the DNA loading process.[37] However, citrate-capped AuNPs are not stable in a high ionic strength environment and are prone to irreversible aggregation. Hence, salt must be introduced gradually with increments of 10−50 mM to reach final concentration typically >300 mM. Following each increment, the mixture should be incubated for a couple of hours, which is troublesome and time-consuming. Another limitation of loading thiolated DNA on AuNPs is the time-consuming aging process to allow maximum loading of DNA, which usually takes an entire day. Although sonication or heating may accelerate the DNA loading process, overnight incubation is still required.[38] Additionally, there may be significant nonspecific adsorption of ssDNA by interaction of the AuNPs via the amine groups of nucleotides,[18] which can largely compromise the loading of thiolated DNA and the recognition ability. Mercaptohexanol (MCH) can be applied to minimize the nonspecific adsorption, so that only the sulfur−gold bond interaction exists.[39,40] However, because excessive displacement of the thiolated DNA by MCH from AuNP surface may result in destabilization of AuNPs, accurate control

Received: June 26, 2014
Accepted: September 4, 2014
Published: September 4, 2014

of MCH concentration and reaction time is required.[39,40] Finally, the procedures do not perform well for large AuNPs, as even more salt addition steps are required.[41,42] Although large AuNPs can be functionalized in the presence of surfactants, such as sodium dodecyl sulfate,[31] gradual addition of salt is still required, extending the process time to an entire day.

To address these issues, a number of alternate conjugation schemes have been proposed. For example, a nonionic fluorosurfactant was reported to assist loading thiolated DNA on AuNPs in 2 h.[43] By this method, AuNPs could be well dispersed in aqueous solution with 1 M NaCl, avoiding the tedious steps of adding NaCl incrementally. However, fluorinated surfactants are cytotoxic, precluding biological applications of AuNPs.[44,45] In addition, Zhang and co-workers elegantly demonstrated that thiolated DNA could be quantitatively attached to AuNPs in a few minutes at pH 3,[46] but this method is not suitable for large nanoparticles, for which high particle concentration or sonication was still needed to assist the DNA attachment process.[47] Moreover, serious nonspecific adsorption of DNA nucleotides may occur.[48] Later, Zhang and co-workers reported a novel depletion method to stabilize AuNPs in extreme ionic strength and pH environments.[49] The AuNPs are stabilized by crowded polymers, but the surfaces are still accessible, and thiolated DNA can attach to AuNPs in 2 h. However, the method is inconvenient, and nonspecific adsorption of DNA nucleotides on AuNPs may still exist.

In this paper, we propose a novel approach for loading thiolated DNA on gold nanoparticles without the tedious and time-consuming salt-addition processes and aging steps. AuNPs with different sizes can be stabilized by mPEG-SH in the presence of Tween 20, where mPEG-SH sterically protects most parts of the AuNP surface and Tween 20 acts as an assisting reagent to protect the residual space. A high concentration of NaCl can be directly added to the solution and the DNA loading process can be completed in 1.5 h, eliminating the labor-intensive gradual salt addition and time-consuming aging processes, while minimizing nonspecific adsorption of DNA nucleotides. This approach provides a new way to stabilize AuNPs for rapid and facile loading of thiolated DNA on AuNPs and will find wide applications in many areas requiring DNA–AuNPs, such as diagnosis, therapy, and imaging.

EXPERIMENTAL SECTION

Materials and Reagents. All the DNA sequences (Table 1) were synthesized on a PolyGen Column 12 DNA synthesizer (PolyGen GmbH, Germany), and all DNA synthesis reagents were purchased from Glen Research (Sterling, VA, USA). $HAuCl_4 \cdot 4H_2O$ and Triton X-100 were supplied by Sinopharm Chemical Reagent Co., Ltd. (Shanghai, China). Pluronic F-127 was obtained from Sigma-Aldrich (St. Louis, MO, USA). Tween 20 and Tween 80 were purchased from Xilong Chemical Co., Ltd. (Guangdong, China). Sodium dodecyl sulfate (SDS) was obtained from J&K Chemical Technology (Guangdong, China). 2-Mercaptoethanol was purchased from Xiya Reagent Company Ltd. (Chengdu, China). mPEG-SH (MW ~750 Da), mPEG-SH (MW ~5 kDa), and mPEG-SH (MW ~20 kDa) were purchased from JenKem Technology Co., Ltd. (Beijing, China).

Table 1. Sequences Used in This Study[a]

name	sequence (5′ to 3′)
DNA1	TAG GAA TAG TTA TA A $(A)_{10}$ -SH
DNA2	TTA TAA CTA TTC CTA $(A)_{10}$-SH
DNA3	CGC ATT CAG GAT T(FAM)-SH
DNA4	CGC ATT CAG GAT T(TMR)-SH
DNA5	CGC ATT CAG GAT $(A)_{20}$T(FAM)-SH
DNA6	ATT GAC CGC TGT GTG ACG CAA CAC TCA A$(T)_{13}$ T(FAM)-SH
DNA7	ATC CTG AAT GCG-FAM

[a]T(FAM) and T(TMR) represent FAM and TMR labeled on T base, respectively.

Synthesis of 13- and 55-nm Gold Nanoparticles. AuNPs with an average diameter of 13 and 55 nm were synthesized by reduction of $HAuCl_4$ with sodium citrate.[50] All glassware used was thoroughly washed with freshly prepared aqua regia (HNO_3/HCl = 1:3) and then rinsed extensively with deionized water. Chloroauric acid (0.01 wt %, 100 mL) was added to a round-bottom flask and boiled with stirring and refluxing. Then 1 mL of 3 wt % sodium citrate (0.7 mL of 1 wt % sodium citrate for 55 nm AuNPs) was quickly added to the boiling solution. The solution was maintained at the boiling point with continuous stirring for 30 min. The solution was allowed to cool to room temperature and stored in the dark until used. UV–vis absorption spectra, photography, and TEM were used to characterize the synthesized AuNPs (Supporting Information (SI) Figure S1). The concentration of AuNPs was determined by UV–vis absorbance based on the reported extinction coefficient of 2.46×10^8 M^{-1} cm^{-1} for 13-nm AuNPs and 2.97×10^{10} M^{-1} cm^{-1} for 55-nm AuNPs.[1] The concentrations of AuNPs synthesized by this method were about 2.5 nM for 13-nm AuNPs and 0.025 nM for 55-nm AuNPs.

Attaching Thiolated DNA to Gold Nanoparticles. To 1 mL of 2.5 nM 13-nm AuNPs solution, 10 μL of 1 wt % Tween 20 and 50 μL of 4 μM mPEG-SH (MW ~5 kDa) were added. After brief mixing, 8 μL of 100 μM thiolated DNAs was added to the mixture and NaCl was added to reach a final concentration of 800 mM. After aging for 60 min at room temperature, excess reagents were removed via centrifugation at 14 000 rpm for 10 min. The precipitate was washed three times with PBST solution (10 mM Na_2HPO_4, 137 mM NaCl, and 2.7 mM KCl, 0.01 wt % Tween 20, pH 7.4) by repetitive centrifugation and dispersion. For comparison, a previously reported method was also used to load thiolated DNA on AuNPs over a 16-h period.[51]

Quantification of DNA Loaded on Gold Nanoparticles. Fluorophore-labeled thiolated DNA was used to quantify the number of oligonucleotides loaded on each particle. After attaching AuNP, the fluorophore-labeled thiolated DNA was cleaved from the purified DNA–AuNPs using aqueous mercaptoethanol as described in previously reported procedures.[52] Briefly, the purified fluorophore-labeled oligonucleotide-modified AuNPs were dispersed in PBST solution and mercaptoethanol was added to the mixture to reach a final concentration of 20 mM. After 5 h incubation at room temperature with continuous mixing, the solution containing displaced oligonucleotides was separated from the AuNPs by centrifugation. To determine the concentration of oligonucleotides, fluorescence measurements were carried out on an RF-5301-PC fluorescence spectrophotometer (Shimadzu, Japan). The emission spectra were obtained by exciting the samples at 497 nm and scanning the emission from 510 to 700 nm in steps of 1 nm. The standard curve was prepared by measuring the fluorescence of different concentrations of fluorophore-labeled DNA. Then, the fluorescence intensity of the supernatant was measured and compared to the standard curve. The number of oligonucleotides on each particle was calculated by dividing the concentration of fluorescent oligonucleotides by the concentration of nanoparticles.

X-ray Photoelectron Spectroscopy. The ligands on the surface of AuNPs were analyzed by X-ray photoelectron spectroscopy (XPS), using a Physical Electronics PHI Quantum 2000 system. All reported values of electron binding energy were calibrated with respect to the principal peak of C_{1s} at 284.5 eV as an internal standard.

Thermal Denaturation of Gold Nanoparticle Assembly. UV melting curves of two complementary thiolated DNA sequences before and after attaching to AuNPs were monitored at 260 nm using a UV–vis spectrophotometer (Agilent 8453, USA) with a temperature

control device (Agilent 89090A). A 200-μL sample of 2.5 nM 13-nm DNA1–AuNPs was mixed with the same amount of 13-nm DNA2–AuNPs in a cuvette. The absorbance changes were recorded from 10 to 70 °C at 1 °C min^{-1}.

Preparation of Gold Nanoparticle Assemblies. The 55-nm AuNPs and 13-nm AuNPs were decorated with DNA1 and DNA2 by the method described above, respectively. The as-prepared DNA–AuNPs were dispersed in PBS solution (10 mM Na_2HPO_4, 137 mM NaCl, and 2.7 mM KCl, pH 7.4). Then 50 μL of 0.25 nM 55-nm DNA1–AuNPs and 50 μL of 25 nM 13-nm DNA2–AuNPs were mixed and incubated at 37 °C for 12 h. The free DNA–AuNPs were removed by three rounds of centrifugation and resuspension in PBS buffer. Aliquots of the AuNP assemblies were taken for TEM analysis (TECNAI F30).

Cytotoxicity Assay. HeLa cells were chosen as the target cells to perform the cytotoxicity assay. HeLa cells growing in log phase were seeded into a 96-well cell-culture plate at 1×10^4/well and cultured in 80 μL of DMEM containing penicillin, streptomycin, and 10% FBS. DNA–AuNPs synthesized by the conventional method or the mPEG-SH-assisted method were gradually diluted to 50, 10, 2, 0.4, and 0 nM with DMEM cell medium. Then, 20-μL aliquots of different concentrations of AuNPs/DMEM solution were applied to HeLa cells and cultured for 24 h. The in vitro cytotoxicity of DNA–AuNPs was evaluated using a standard MTT (methyl thiazolyl tetrazolium) assay.

RESULTS AND DISCUSSION

Working Principle of mPEG-SH-Assisted Attaching of Thiolated DNA to AuNPs. Citrate-stabilized AuNPs of different sizes are stable in an aqueous solution with low ionic strength and narrow pH range, but irreversible aggregation of AuNPs will occur in the presence of NaCl over 50 mM. Because citrate-stabilized AuNPs are negatively charged and the charge strength increases with the attachment of negatively charged DNA, a time-consuming and labor-intensive process of incremental NaCl addition has been used to screen the charge repulsion between DNA and AuNPs before loading high-density thiolated DNA on AuNPs (Figure 1A).[51] To address this problem, Zu proposed a nonionic

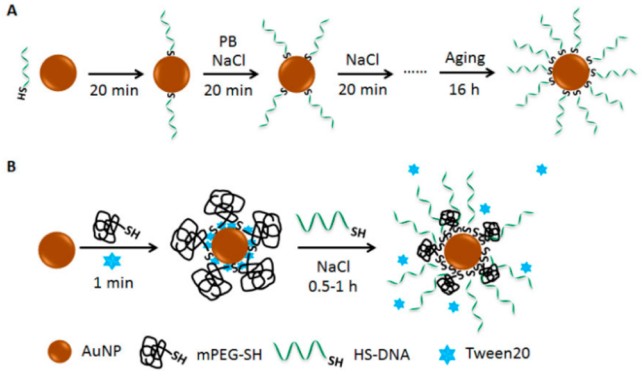

Figure 1. Working principle and procedures of current standard method (A) and mPEG-SH-assisted method (B) to load thiolated DNA on AuNPs (size not to scale).

fluorosurfactant method to increase the stability of AuNPs,[43] but the fluorosurfactant is cytotoxic. Zhang developed a pH-assisted method to reduce the charge repulsion between AuNPs and DNA, but it was not suitable for large AuNPs.[46] Here, we propose a mPEG-SH-assisted method to stabilize AuNPs in the presence of Tween 20. The working principle of our strategy is illustrated in Figure 1B. To stabilize AuNPs, Tween 20 and mPEG-SH (MW ~5 kDa) are first added to the AuNP solution to reach a final concentration of 0.01 wt % and 200 nM, respectively. After brief mixing, thiolated DNA is added to the mixture, directly followed by NaCl, with the final concentration of 800 nM and 800 mM, respectively. The previous weakly adsorbed Tween 20 will be displaced by thiolated DNA during the DNA loading process. After incubation for 1 h, the free DNA is removed by centrifugation. AuNPs of different sizes stabilized by this method can be stably dispersed in high ionic strength (0.8 M NaCl) solution and over a wide pH range (from pH 1 to 13). The thiolated DNA can be attached to AuNPs quantitatively and DNA–AuNPs are stable at room temperature for more than 2 weeks.

Stability of mPEG-SH Protected Gold Nanoparticles in the Presence of Tween 20. To demonstrate the synergistic effect of Tween 20 and mPEG-SH in protecting AuNPs from aggregation, the protecting abilities of mPEG-SH and Tween 20 were investigated individually. First, different concentrations of mPEG-SH were added to 2.5 nM 13-nm AuNPs (SI Figure S2A), and after 20 min incubation, different concentrations of NaCl were applied to the mixture. The results showed that 1000 nM mPEG-SH can protect 13-nm AuNPs in the presence of up to 800 mM NaCl. This indicates that sufficient mPEG-SH had attached to the AuNP surface to create steric hindrance to protect AuNPs from aggregation, but the steric hindrance may also compromise the DNA loading capacity on AuNPs. Second, we tested the protecting ability of Tween 20. As shown in SI Figure S2B, attaching to AuNP surface by weak physical adsorption, Tween 20 cannot stabilize AuNPs in a high ionic strength environment. Herein, we combined the advantages of the large steric hindrance of mPEG-SH and the weak adsorption property of Tween 20 to stabilize AuNPs in a high ionic strength environment. As shown in Figure 2 and SI

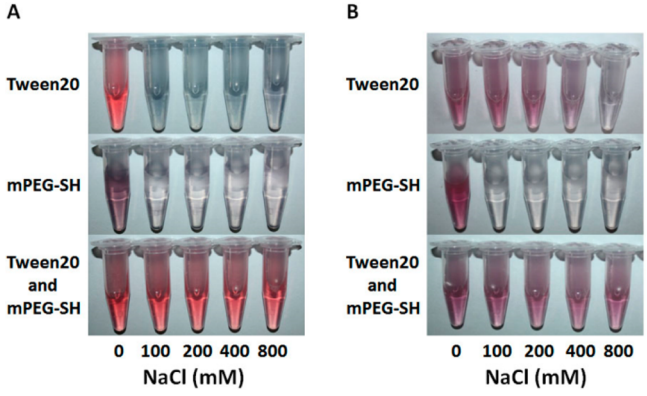

Figure 2. Dispersibility of 13-nm (A) and 55-nm (B) AuNPs protected by different protective reagents followed by adding different concentrations of NaCl. The concentrations of Tween 20 and mPEG-SH applied for 13-nm AuNP (2.5 nM) were 0.01 wt % and 200 nM, respectively. The concentrations of Tween 20 and mPEG-SH applied for 55-nm AuNP (0.025 nM) were 0.01 wt % and 40 nM, respectively.

Figure S3, 0.01 wt % Tween 20 and 200 nM mPEG-SH were applied to 2.5 nM citrate-capped 13-nm AuNPs before adding different concentrations of NaCl. Irreversible aggregation of AuNPs occurred in 100 mM NaCl in the presence of Tween 20 or mPEG-SH alone. In contrast, AuNPs were stably dispersed in the presence of 800 mM NaCl with both Tween 20 and mPEG-SH present. In the case of 55 nm AuNPs, 0.01 wt % Tween 20 and 40 nM mPEG-SH were used instead, because of the lower concentration of the 55-nm AuNPs (0.025 nM).

Similarly, 0.01 wt % Tween 20 or 40 nM mPEG-SH alone were not able to protect 55-nm AuNPs from aggregation in the presence of 400 mM NaCl, but AuNPs were well dispersed in 800 mM NaCl when Tween 20 and mPEG-SH were both present. These results show that AuNPs can be protected by the synergistic effect of Tween 20 and mPEG-SH.

Several mechanisms have been proposed to explain the protective properties of different materials on AuNPs. First, charge stabilization is the most widely recognized effect, which was proposed to interpret the protective properties of citrate on AuNPs. For AuNPs prepared by the citrate reduction method, citrate ions are believed to adsorb onto the surface of AuNPs to render a negatively charged surface for charge stabilization.[53] The second mechanism is depletion stabilization. Nanoparticles may experience a depletion force originating from the excluded volume effect of the polymer when they are dispersed in a nonadsorbing polymer solution.[49,54] The third mechanism is steric stabilization. Polyethylene glycol (PEG) is considered to be weakly adsorbed on gold nanoparticle surfaces,[54] and it acts as a steric stabilizer to stabilize AuNPs by preventing them from touching each other. On the basis of the mechanisms proposed above, it is highly possible that mPEG-SH was linked to the AuNP surface by a sulfur−gold bond. The PEG acted as a steric stabilizer to protect most parts of AuNP surface, and Tween 20 played an assisting role in protecting the residual space of AuNP surface.

Effect of Different Surfactants and Different Sizes of mPEG-SH on Stabilizing Gold Nanoparticles. After demonstrating the synergistic effect of Tween 20 and mPEG-SH in protecting AuNPs, the synergistic effect between other kinds of surfactants and mPEG-SH was investigated (SI Figure S4). In these experiments, we employed a positively charged surfactant, cetyltrimethylammonium bromide (CTAB), a negatively charged surfactant, sodium dodecyl sulfate (SDS), and three nonionic surfactants: pluronic F127, Tween 80, and Triton X-100. These surfactants were chosen according to their charge states and molecular structures to compare the effects of different kinds of surfactants in stabilizing AuNPs and confirm the mechanism of synergistic effect. Different concentrations of surfactants were added to citrate-capped 13-nm AuNPs with 200 nM mPEG-SH. After brief mixing, the concentration of NaCl was adjusted to 800 mM. All tested surfactants except SDS exhibited a synergistic effect with mPEG-SH in stabilizing AuNPs, but the minimum concentration of surfactant required differed, probably due to the different chemical structures of surfactants resulting in the difference in affinity and steric hindrance on AuNPs. We obtained similar results with 55-nm AuNPs, with all surfactants except SDS having a synergistic effect with mPEG-SH in stabilizing AuNPs. The experiments above confirmed the necessity of Tween 20 (or other nonionic surfactant or CTAB) in protecting AuNPs from aggregation.

Next, we studied the stability of AuNPs as a function of mPEG-SH with different sizes. Tween 20 of 0.01 wt % and different concentrations of mPEG-SH with different sizes were added to 1 mL of 2.5 nM citrate-capped 13-nm AuNPs aqueous solution, and then the concentration of NaCl was adjusted to 800 mM. An immediate color change to blue and then to colorless was observed for AuNPs that were not well protected. As shown in Figure 3A and SI Figure S5A, the minimum concentration of mPEG-SH needed to stabilize 13-nm AuNPs decreased with the increasing of mPEG-SH size, due to the larger steric hindrance provided by each mPEG-SH. In the case of 55-nm AuNPs (Figure 3B and SI Figure S5B), similar results

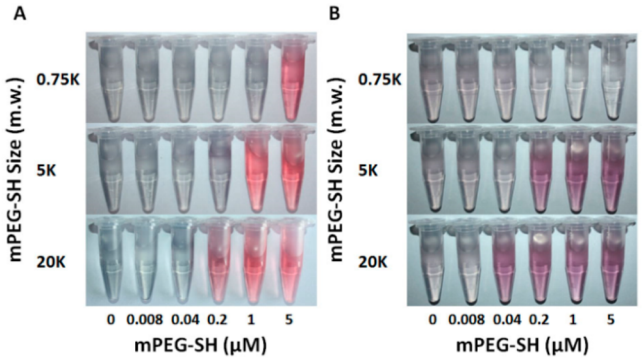

Figure 3. Photograph of 13-nm (A) and 55-nm (B) AuNPs protected by 0.01 wt % Tween 20 and different concentrations of mPEG-SH with different sizes followed by adding 800 mM NaCl.

were obtained, but 55-nm AuNPs could not be stabilized by the smallest size mPEG-SH (MW 750 Da) even at 5 μM concentration. We suspected that the size of mPEG-SH (MW 750 Da) is smaller than the London interaction[55−58] range of 55-nm AuNPs and steric stabilization cannot be achieved. Moreover, the incubation time between mPEG-SH and AuNPs in the presence of Tween 20 was also investigated, and we found that just brief mixing of mPEG-SH with AuNPs was enough to stabilize AuNPs in 800 mM NaCl solution (SI Figure S6A) and over a wide range of pH (SI Figure S6B).

Surface Protecting Process Confirmed by XPS. To confirm the mechanism we proposed, the process of AuNP stabilization at each step was monitored by X-ray photoelectron spectroscopy (XPS). The presence of elemental gold and the exchange of capping reagents were confirmed by XPS (SI Figure S7). AuNPs synthesized by the citrate reduction method are capped with citrate and a strong O_{1s} peak and a week C_{1s} peak can be found at 531 and 284 eV, respectively. By displacing citrate with Tween 20, the C_{1s} peak increased significantly, while the O_{1s} peak remained almost the same, due to the high percentage of carbon species attached to the surface of AuNPs. By further attaching mPEG-SH on AuNPs, some of the Tween 20 molecules loaded on AuNPs were displaced by mPEG-SH, so that both the C_{1s} and O_{1s} peaks decreased. In addition, significant differences could also be observed in C_{1s} high-resolution XPS spectra (Figure 4). The carbon species from citrate capped AuNPs were hydrocarbons (C−C and C−H, peak 1) and carboxyl carbon (O−C═O, peak 3) with binding energies of ∼284.5 and ∼288.5 eV, respectively. There was also a peak at 285.5 eV, corresponding to carbon bound to oxygen (C−OH, peak 2) in the form of oxidized adventitious carbon.[59] The carbon species from Tween 20 or both Tween 20 and mPEG-SH capped AuNPs were hydrocarbons (C−C and C−H, peak 1) and the carbon bound to oxygen (peak 2) showed characteristic binding energies of ∼284.5 and ∼285.5 eV. As summarized in Figure 4D, the peak for carbon bound to oxygen (peak 2) increased significantly and the peak for the carboxyl carbon (peak 3) decreased as the citrate was displaced by Tween 20. Both carbon bound to oxygen (peak 2) and carboxyl carbon (peak 3) decreased when mPEG-SH was further added to decorate AuNPs and displace Tween 20 from the AuNP surface. These results confirmed that both Tween 20 and mPEG-SH attached to the surface of AuNP to provide a synergistic effect in protecting AuNP form aggregation.

Effects of Different Factors on DNA Loading Capacity. After confirming the stabilization of AuNPs by mPEG-SH in

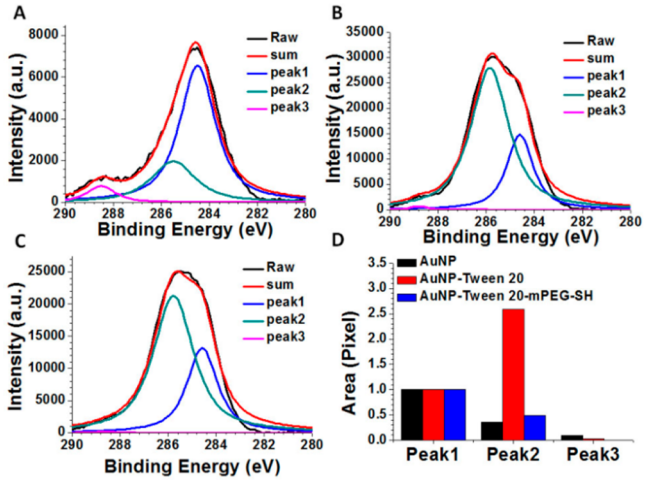

Figure 4. High-resolution C_{1s} XPS spectra of (A) citrate capped AuNPs, (B) Tween 20 capped AuNPs, and (C) Tween 20 and mPEG-SH capped AuNPs. (D) Corresponding normalized peak intensity of different types of AuNPs.

the presence of Tween 20, different factors that affect DNA loading capacity were investigated. First, we investigated the effect of different kinds of surfactants including Tween 20, Tween 80, pluronic F127, and Triton X-100. The number of DNAs loaded on each 13-nm AuNP was almost the same in the presence of 0.01 wt % of different surfactants (Figure 5A). In

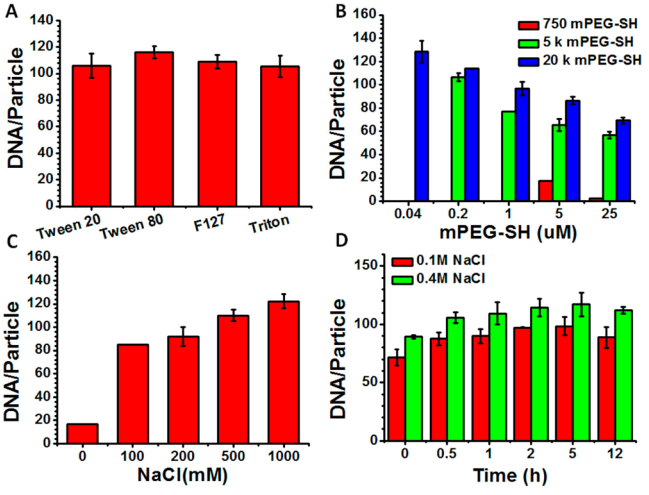

Figure 5. Factors affecting DNA loading capacity on 13-nm AuNPs: (A) types of surfactants; (B) concentrations of mPEG-SH with different sizes; the minimum concentrations of mPEG-SH were determined by their abilities to stabilize AuNPs; (C) NaCl concentrations; and (D) aging time.

contrast, the DNA loading capacity would be affected by the increasing concentration of Tween 20 (SI Figure S8A). We then considered the effect of the size and concentration of mPEG-SH on DNA loading capacity. As the minimum required concentrations of mPEG-SH with different sizes were different, the minimum concentrations of mPEG-SH we investigated were 5, 0.2, and 0.04 μM for mPEG-SH (MW 750 Da), mPEG-SH (MW 5 kDa), and mPEG-SH (MW 20 kDa), respectively. As shown in Figure 5B, the number of DNAs on each 13-nm AuNP increased with the increasing of mPEG-SH size and decreasing of mPEG-SH concentration. Because the number of mPEG-SH attached to AuNPs decreased as the size of mPEG-SH increased, the residual space on the AuNP surface increased, thereby increasing the number of DNAs loaded. Similarly, the DNA loading capacity decreased with increasing concentration of mPEG-SH, since more space was occupied by mPEG-SH. Moreover, we found that the number of DNAs loaded on each nanoparticle increased with increasing concentration of NaCl (Figure 5C) and HS-DNA (SI Figure S8B). As for 55-nm AuNPs, the concentration of Tween 20 would not affect DNA loading capacity (SI Figure S8C), but increasing concentration of mPEG-SH would reduce the number of DNA on each 55-nm AuNP (SI Figure S8D). Finally, we investigated the time needed to finish the DNA loading process (Figure 5D). After 30 min of aging process, DNA was found saturated on AuNP surface. All steps taken together, the whole DNA loading process could be finished in less than 1 h. To maximize DNA loading, we used 1 h for the aging process, where the whole loading process could be finished within 1.5 h. Therefore, the number of DNAs loaded on each AuNP could easily be controlled by the concentrations of surfactants, mPEG-SH, and NaCl, and by the size of mPEG-SH. The pH-assisted method developed by Zhang[46] avoided the salt addition process and the entire DNA loading process could be finished in 5 min. But we also found that severe nonspecific adsorption of DNA base occurred using the pH-assisted method (SI Figure S9), making the method unsuitable for long-chain thiolated DNA and compromising the hybridization efficiency (SI Figure S10).

Quantitative DNA Loading on AuNPs and Functionality of DNA Conjugated AuNPs. For more advanced applications, it is desirable to load more than one type of DNA on each AuNP. Therefore, different ratios of DNA3 and DNA4 were used to functionalize AuNPs (Figure 6A). The numbers of DNA3 and DNA4 loaded on AuNPs were proportional to the ratio applied to the AuNP solution. To ensure that DNA

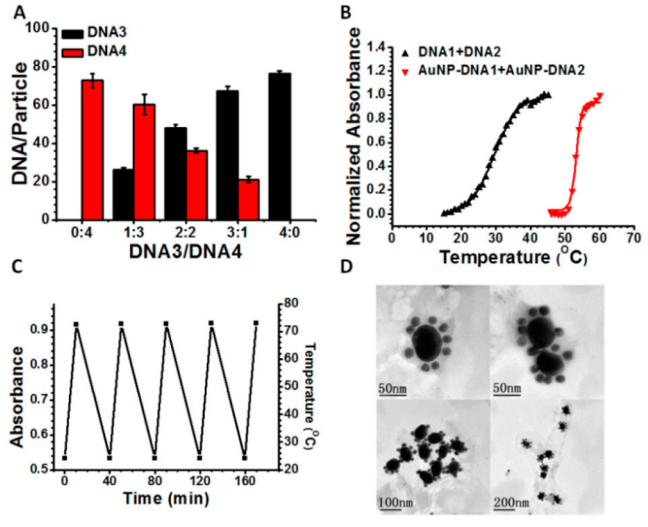

Figure 6. (A) Attachment of two HS-DNAs (DNA3 and DNA4) on 13-nm AuNPs with different ratios. (B) Melting temperature of complementary HS-DNA (DNA1 and DNA2) before and after loading on AuNPs. Triangle and line correspond to experimental data and simulation results, respectively. (C) Reversible assembly of DNA1–AuNPs and DNA2–AuNPs at 25 and 75 °C in PBS buffer. (D) Representative TEM images of 55-nm DNA1–AuNPs assembled with 13-nm DNA2–AuNPs.

dx.doi.org/10.1021/am504139d | ACS Appl. Mater. Interfaces 2014, 6, 16800–16807

loaded on AuNPs can still function well, we investigated the melting profiles of DNA–AuNPs and tested the DNA-directed assembly of AuNPs. The melting profiles of 13-nm DNA1–AuNPs and 13-nm DNA2–AuNPs were obtained by monitoring the absorbance at 260 nm as a function of temperature. As shown in Figure 6B, the melting temperature of DNA1 and DNA2 on AuNPs increased almost 25 °C compared to that of pure DNA, and the melting profile exhibited an extremely sharp transition which is convincing evidence of a high DNA density on AuNPs.[37] Moreover, assembly and disassembly of DNA–AuNPs between 25 and 75 °C were reversible even after 5 cycles (Figure 6C). To further confirm the assembly of AuNPs functionalized with complementary DNA, 55-nm DNA1–AuNPs and 13-nm DNA2–AuNPs were fabricated separately by the mPEG-SH-assisted method, and then they were allowed to hybridize at 37 °C for 12 h. On average, the AuNP assemblies were composed of one 55-nm AuNP and eight 13-nm AuNPs (Figure 6D). As a comparison, 55-nm DNA1–AuNPs did not hybridize with the noncomplementary 13-nm DNA3–AuNPs and could not form AuNP assemblies (SI Figure S11). The experiments above confirm the functionality of DNA–AuNPs fabricated by this method.

Long-Term Stability and Cytotoxicity of DNA–AuNPs. High stability over time is always a basic requirement for functionalized materials. Therefore, the time-dependent stability of DNA–AuNPs prepared by the mPEG-SH-assisted method and by a current standard protocol[51] was compared. The 13-nm AuNPs were decorated with DNA3 by the two different protocols and stored in the dark at room temperature. The AuNP stabilities were evaluated by dispersibility in water. As shown in Figure 7A and SI Figure S12, the DNA3–AuNPs

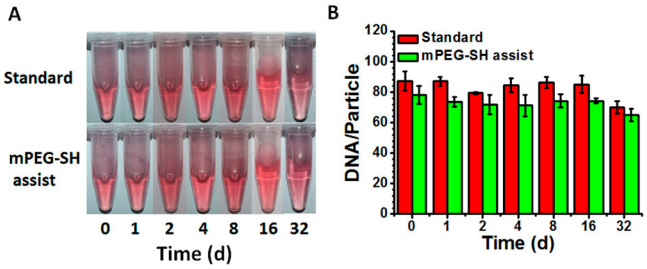

Figure 7. Stability of 13-nm AuNPs functionalized by current standard method and the mPEG-SH-assisted method: (A) dispersibility of AuNPs over time; (B) the number of DNAs loaded on AuNPs over time.

fabricated by both the standard method[51] and the mPEG-SH-assisted method could be well dispersed for over 2 weeks. To test the loading stability of AuNPs, the number of DNAs attached to the AuNPs was considered. Fluorophore-labeled thiolated DNA was attached to AuNPs by both the standard and the mPEG-SH-assisted method, and the number of DNAs loaded was determined on different days. As shown in Figure 7B, the number of DNAs on DNA–AuNPs fabricated by the standard method was slightly greater than the number on AuNPs fabricated by the mPEG-SH-assisted method. The number of DNAs on each particle remained almost the same for over 2 weeks. The results demonstrated that the long-term stability of DNA–AuNPs fabricated by the mPEG-SH-assisted method was as good as that of DNA–AuNPs fabricated by the current standard method. Thus, rapid processing did not compromise the DNA–AuNP stability.

One of the major challenges for the bioapplication of DNA–AuNPs is the biocompatibility of the material. Hence, the cytotoxicity of DNA–AuNPs prepared by mPEG-SH-assisted method and the current standard method were investigated. Different concentrations of the prepared AuNPs were applied to the cell culture medium. Cells were cultured at 37 °C for 24 h and cell viability was evaluated by MTT assay. As shown in SI Figure S13, the cell viability decreased slightly with an increase of AuNP concentration from 0.1 to 10 nM for both protocols, indicating that the DNA–AuNPs decorated by the mPEG-SH-assisted method bear no extra cytotoxicity and can be directly used for bioanalytical and biomedical applications.

CONCLUSIONS

In conclusion, we demonstrated that different sizes of AuNPs can be stabilized by the synergistic protection effect of surfactant and mPEG-SH over a wide range of pHs and ionic strengths. The minimum required concentration of surfactant differs for each type of surfactant, as different chemical structures result in different affinities. The minimum required concentration of mPEG-SH decreases with increasing size of mPEG-SH due to the larger steric hindrance. The stabilization processes of AuNPs were further confirmed by XPS. On the basis of this finding, we have proposed a novel protocol to load thiolated DNA on AuNPs without the tedious salt addition processes, with the maximum quantity of thiolated DNA loaded achieved within 1.5 h. The number of DNAs loaded on each gold nanoparticle could be easily controlled by the concentrations of mPEG-SH and salt, the size of mPEG-SH, and the aging time. In addition, we observed no effect on hybridization capability, excellent biocompatibility, and long-term stability of DNA–AuNPs. The proposed protocol not only prevents nonspecific adsorption of nucleotide bases of thiolated DNA, but also extends the stability of functionalized AuNPs. The ability to stabilize AuNPs by the synergistic effect of Tween 20 and thiolated PEG offers an exciting new way to simplify the thiolated DNA loading process, and it will greatly extend the application of DNA–AuNPs in nanoscience and biomedicine.

ASSOCIATED CONTENT

Supporting Information

Additional data confirming the synergistic protecting effect of Tween 20 and mPEG-SH, nonspecific adsorption of DNA on gold nanoparticles, assembly and cell viability of DNA–AuNPs. This material is available free of charge via the Internet at http://pubs.acs.org.

AUTHOR INFORMATION

Corresponding Authors

*Tel: (+86) 592-218-7601. Fax: (+86) 592-218-9959. E-mail: cyyang@xmu.edu.cn.

*Tel: (+86) 592-218-4768. Fax: (+86) 592-218-4768. E-mail: kang@xmu.edu.cn.

Notes

The authors declare no competing financial interest.

ACKNOWLEDGMENTS

We thank the National Basic Research Program of China (2010CB732402, 2013CB933703), the National Natural Science Foundation of China (91313302, 21205100,

21275122, 21075104), National Instrumentation Program (2011YQ03012412), the Fundamental Research Funds for the Central Universities (2012121025), NFFTBS(J1310024), and the National Natural Science Foundation for Distinguished Young Scholars of China (21325522) for their financial support.

REFERENCES

(1) Liu, X.; Atwater, M.; Wang, J.; Huo, Q. Extinction Coefficient of Gold Nanoparticles with Different Sizes and Different Capping Ligands. *Colloids Surf., B* **2007**, *58*, 3−7.
(2) Ao, L.; Gao, F.; Pan, B.; He, R.; Cui, D. Fluoroimmunoassay for Antigen Based on Fluorescence Quenching Signal of Gold Nanoparticles. *Anal. Chem.* **2006**, *78*, 1104−1106.
(3) Fan, C.; Wang, S.; Hong, J. W.; Bazan, G. C.; Plaxco, K. W.; Heeger, A. J. Beyond Superquenching: Hyper-Efficient Energy Transfer from Conjugated Polymers to Gold Nanoparticles. *Proc. Natl. Acad. Sci. U. S. A.* **2003**, *100*, 6297−6301.
(4) Li, H.; Rothberg, L. J. DNA Sequence Detection Using Selective Fluorescence Quenching of Tagged Oligonucleotide Probes by Gold Nanoparticles. *Anal. Chem.* **2004**, *76*, 5414−5417.
(5) Wang, H.; Wang, Y.; Jin, J.; Yang, R. Gold Nanoparticle-Based Colorimetric and "Turn-on" Fluorescent Probe for Mercury(II) Ions in Aqueous Solution. *Anal. Chem.* **2008**, *80*, 9021−9028.
(6) Boyen, H. G.; Kaestle, G.; Weigl, F.; Koslowski, B.; Dietrich, C.; Ziemann, P.; Spatz, J. P.; Riethmueller, S.; Hartmann, C.; Moeller, M.; Schmid, G.; Garnier, M. G.; Oelhafen, P. Oxidation-Resistant Gold-55 Clusters. *Science* **2002**, *297*, 1533−1536.
(7) Qian, X.; Peng, X.-H.; Ansari, D. O.; Yin-Goen, Q.; Chen, G. Z.; Shin, D. M.; Yang, L.; Young, A. N.; Wang, M. D.; Nie, S. In Vivo Tumor Targeting and Spectroscopic Detection with Surface-Enhanced Raman Nanoparticle Tags. *Nat. Biotechnol.* **2008**, *26*, 83−90.
(8) Corma, A.; Garcia, H. Supported Gold Nanoparticles as Catalysts for Organic Reactions. *Chem. Soc. Rev.* **2008**, *37*, 2096−2126.
(9) Hill, H. D.; Macfarlane, R. J.; Senesi, A. J.; Lee, B.; Park, S. Y.; Mirkin, C. A. Controlling the Lattice Parameters of Gold Nanoparticle Fcc Crystals with Duplex DNA Linkers. *Nano Lett.* **2008**, *8*, 2341−2344.
(10) Nykypanchuk, D.; Maye, M. M.; van der Lelie, D.; Gang, O. DNA-Guided Crystallization of Colloidal Nanoparticles. *Nature* **2008**, *451*, 549−552.
(11) Park, S. Y.; Lytton-Jean, A. K. R.; Lee, B.; Weigand, S.; Schatz, G. C.; Mirkin, C. A. DNA-Programmable Nanoparticle Crystallization. *Nature* **2008**, *451*, 553−556.
(12) Cui, L.; Ke, G.; Zhang, W. Y.; Yang, C. J. A Universal Platform for Sensitive and Selective Colorimetric DNA Detection Based on Exo III Assisted Signal Amplification. *Biosens. Bioelectron.* **2011**, *26*, 2796−2800.
(13) Chen, Y.; O'Donoghue, M. B.; Huang, Y.-F.; Kang, H.; Phillips, J. A.; Chen, X.; Estevez, M.-C.; Yang, C. J.; Tan, W. A Surface Energy Transfer Nanoruler for Measuring Binding Site Distances on Live Cell Surfaces. *J. Am. Chem. Soc.* **2010**, *132*, 16559−16570.
(14) Chen, J.; Fang, Z.; Lie, P.; Zeng, L. Computational Lateral Flow Biosensor for Proteins and Small Molecules: A New Class of Strip Logic Gates. *Anal. Chem.* **2012**, *84*, 6321−6325.
(15) Zhao, W.; Ali, M. M.; Aguirre, S. D.; Brook, M. A.; Li, Y. Paper-Based Bioassays Using Gold Nanoparticle Colorimetric Probes. *Anal. Chem.* **2008**, *80*, 8431−8437.
(16) Xu, W.; Xue, X.; Li, T.; Zeng, H.; Liu, X. Ultrasensitive and Selective Colorimetric DNA Detection by Nicking Endonuclease Assisted Nanoparticle Amplification. *Angew. Chem., Int. Ed.* **2009**, *48*, 6849−6852.
(17) Storhoff, J. J.; Lucas, A. D.; Garimella, V.; Bao, Y. P.; Mueller, U. R. Homogeneous Detection of Unamplified Genomic DNA Sequences Based on Colorimetric Scatter of Gold Nanoparticle Probes. *Nat. Biotechnol.* **2004**, *22*, 883−887.
(18) Pan, W.; Yang, H.; Zhang, T.; Li, Y.; Li, N.; Tang, B. Dual-Targeted Nanocarrier Based on Cell Surface Receptor and Intracellular MRNA: An Effective Strategy for Cancer Cell Imaging and Therapy. *Anal. Chem.* **2013**, *85*, 6930−6935.
(19) Xiao, Z.; Ji, C.; Shi, J.; Pridgen, E. M.; Frieder, J.; Wu, J.; Farokhzad, O. C. DNA Self-Assembly of Targeted near-Infrared-Responsive Gold Nanoparticles for Cancer Thermo-Chemotherapy. *Angew. Chem., Int. Ed.* **2012**, *51*, 11853−11857.
(20) Khlebtsov, B.; Zharov, V.; Melnikov, A.; Tuchin, V.; Khlebtsov, N. Optical Amplification of Photothermal Therapy with Gold Nanoparticles and Nanoclusters. *Nanotechnology* **2006**, *17*, 5167−5179.
(21) Li, Y.; Wark, A. W.; Lee, H. J.; Corn, R. M. Single-Nucleotide Polymorphism Genotyping by Nanoparticle-Enhanced Surface Plasmon Resonance Imaging Measurements of Surface Ligation Reactions. *Anal. Chem.* **2006**, *78*, 3158−3164.
(22) Li, N.; Chang, C.; Pan, W.; Tang, B. A Multicolor Nanoprobe for Detection and Imaging of Tumor-Related MRNAs in Living Cells. *Angew. Chem., Int. Ed.* **2012**, *51*, 7426−7430.
(23) Kang, B.; Mackey, M. A.; El-Sayed, M. A. Nuclear Targeting of Gold Nanoparticles in Cancer Cells Induces DNA Damage, Causing Cytokinesis Arrest and Apoptosis. *J. Am. Chem. Soc.* **2010**, *132*, 1517−1519.
(24) Jin, Y.; Li, H.; Bai, J. Homogeneous Selecting of a Quadruplex-Binding Ligand-Based Gold Nanoparticle Fluorescence Resonance Energy Transfer Assay. *Anal. Chem.* **2009**, *81*, 5709−5715.
(25) Skewis, L. R.; Reinhard, B. M. Spermidine Modulated Ribonuclease Activity Probed by RNA Plasmon Rulers. *Nano Lett.* **2008**, *8*, 214−220.
(26) Cao, Y. C.; Jin, R.; Mirkin, C. A. Nanoparticles with Raman Spectroscopic Fingerprints for DNA and RNA Detection. *Science* **2002**, *297*, 1536−1540.
(27) Han, G.; You, C.-C.; Kim, B.-j.; Turingan, R. S.; Forbes, N. S.; Martin, C. T.; Rotello, V. M. Light-Regulated Release of DNA and Its Delivery to Nuclei by Means of Photolabile Gold Nanoparticles. *Angew. Chem., Int. Ed.* **2006**, *45*, 3165−3169.
(28) Huschka, R.; Zuloaga, J.; Knight, M. W.; Brown, L. V.; Nordlander, P.; Halas, N. J. Light-Induced Release of DNA from Gold Nanoparticles: Nanoshells and Nanorods. *J. Am. Chem. Soc.* **2011**, *133*, 12247−12255.
(29) Salem, A. K.; Searson, P. C.; Leong, K. W. Multifunctional Nanorods for Gene Delivery. *Nat. Mater.* **2003**, *2*, 668−671.
(30) Rosi, N. L.; Giljohann, D. A.; Thaxton, C. S.; Lytton-Jean, A. K. R.; Han, M. S.; Mirkin, C. A. Oligonucleotide-Modified Gold Nanoparticles for Intracellular Gene Regulation. *Science* **2006**, *312*, 1027−1030.
(31) Hurst, S. J.; Lytton-Jean, A. K. R.; Mirkin, C. A. Maximizing DNA Loading on a Range of Gold Nanoparticle Sizes. *Anal. Chem.* **2006**, *78*, 8313−8318.
(32) Zhang, J.; Song, S.; Zhang, L.; Wang, L.; Wu, H.; Pan, D.; Fan, C. Sequence-Specific Detection of Femtomolar DNA Via a Chronocoulometric DNA Sensor (CDS): Effects of Nanoparticle-Mediated Amplification and Nanoscale Control of DNA Assembly at Electrodes. *J. Am. Chem. Soc.* **2006**, *128*, 8575−8580.
(33) Liu, Y.-C.; Li, Y.-J.; Huang, C.-C. Information Derived from Cluster Ions from DNA-Modified Gold Nanoparticles under Laser Desorption/Ionization: Analysis of Coverage, Structure, and Single-Nucleotide Polymorphism. *Anal. Chem.* **2013**, *85*, 1021−1028.
(34) Cao, Y. C.; Jin, R.; Nam, J.-M.; Thaxton, C. S.; Mirkin, C. A. Raman Dye-Labeled Nanoparticle Probes for Proteins. *J. Am. Chem. Soc.* **2003**, *125*, 14676−14677.
(35) Jang, B.; Park, J.-Y.; Tung, C.-H.; Kim, I.-H.; Choi, Y. Gold Nanorod− Photosensitizer Complex for near-Infrared Fluorescence Imaging and Photodynamic/Photothermal Therapy in Vivo. *ACS Nano* **2011**, *5*, 1086−1094.
(36) Wang, J.; You, M.; Zhu, G.; Shukoor, M. I.; Chen, Z.; Zhao, Z.; Altman, M. B.; Yuan, Q.; Zhu, Z.; Chen, Y. Photosensitizer−Gold Nanorod Composite for Targeted Multimodal Therapy. *Small* **2013**, *9*, 3678−3684.
(37) Storhoff, J. J.; Elghanian, R.; Mucic, R. C.; Mirkin, C. A.; Letsinger, R. L. One-Pot Colorimetric Differentiation of Polynucleo-

tides with Single Base Imperfections Using Gold Nanoparticle Probes. *J. Am. Chem. Soc.* **1998**, *120*, 1959−1964.
(38) Hurst, S. J.; Lytton-Jean, A. K.; Mirkin, C. A. Maximizing DNA Loading on a Range of Gold Nanoparticle Sizes. *Anal. Chem.* **2006**, *78*, 8313−8318.
(39) Park, S.; Brown, K. A.; Hamad-Schifferli, K. Changes in Oligonucleotide Conformation on Nanoparticle Surfaces by Modification with Mercaptohexanol. *Nano Lett.* **2004**, *4*, 1925−1929.
(40) Zhao, W.; Chiuman, W.; Brook, M. A.; Li, Y. Simple and Rapid Colorimetric Biosensors Based on DNA Aptamer and Noncrosslinking Gold Nanoparticle Aggregation. *ChemBioChem* **2007**, *8*, 727−731.
(41) Jin, R.; Wu, G.; Li, Z.; Mirkin, C. A.; Schatz, G. C. What Controls the Melting Properties of DNA-Linked Gold Nanoparticle Assemblies? *J. Am. Chem. Soc.* **2003**, *125*, 1643−1654.
(42) Liu, J.; Lu, Y. Accelerated Color Change of Gold Nanoparticles Assembled by DNAzymes for Simple and Fast Colorimetric Pb2+ Detection. *J. Am. Chem. Soc.* **2004**, *126*, 12298−12305.
(43) Zu, Y.; Gao, Z. Facile and Controllable Loading of Single-Stranded DNA on Gold Nanoparticles. *Anal. Chem.* **2009**, *81*, 8523−8528.
(44) Moody, C. A.; Field, J. A. Perfluorinated Surfactants and the Environmental Implications of Their Use in Fire-Fighting Foams. *Environ. Sci. Technol.* **2000**, *34*, 3864−3870.
(45) Courrier, H. M.; Krafft, M. P.; Butz, N.; Porte, C.; Frossard, N.; Remy-Kristensen, A.; Mely, Y.; Pons, F.; Vandamme, T. F. Evaluation of Cytotoxicity of New Semi-Fluorinated Amphiphiles Derived from Dimorpholinophosphate. *Biomaterials* **2002**, *24*, 689−696.
(46) Zhang, X.; Servos, M. R.; Liu, J. Instantaneous and Quantitative Functionalization of Gold Nanoparticles with Thiolated DNA Using a pH-Assisted and Surfactant-Free Route. *J. Am. Chem. Soc.* **2012**, *134*, 7266−7269.
(47) Zhang, X.; Gouriye, T.; Göeken, K.; Servos, M. R.; Gill, R.; Liu, J. Toward Fast and Quantitative Modification of Large Gold Nanoparticles by Thiolated DNA: Scaling of Nanoscale Forces, Kinetics, and the Need for Thiol Reduction. *J. Phys. Chem. C* **2013**, *117*, 15677−15684.
(48) Zhang, X.; Liu, B.; Dave, N.; Servos, M. R.; Liu, J. Instantaneous Attachment of an Ultrahigh Density of Nonthiolated DNA to Gold Nanoparticles and Its Applications. *Langmuir* **2012**, *28*, 17053−17060.
(49) Zhang, X.; Servos, M. R.; Liu, J. Ultrahigh Nanoparticle Stability against Salt, pH, and Solvent with Retained Surface Accessibility via Depletion Stabilization. *J. Am. Chem. Soc.* **2012**, *134*, 9910−9913.
(50) Frens, G. Controlled Nucleation for the Regulation of the Particle Size in Monodisperse Gold Suspensions. *Nature* **1973**, *241*, 20−22.
(51) Song, S.; Liang, Z.; Zhang, J.; Wang, L.; Li, G.; Fan, C. Gold-Nanoparticle-Based Multicolor Nanobeacons for Sequence-Specific DNA Analysis. *Angew. Chem., Int. Ed.* **2009**, *48*, 8670−8674.
(52) Demers, L. M.; Mirkin, C. A.; Mucic, R. C.; Reynolds, R. A.; Letsinger, R. L.; Elghanian, R.; Viswanadham, G. A Fluorescence-Based Method for Determining the Surface Coverage and Hybridization Efficiency of Thiol-Capped Oligonucleotides Bound to Gold Thin Films and Nanoparticles. *Anal. Chem.* **2000**, *72*, 5535−5541.
(53) Turkevich, J. Colloidal Gold. Part II. *Gold Bull.* **1985**, *18*, 125−131.
(54) Lang, N.; Liu, B.; Zhang, X.; Liu, J. Dissecting Colloidal Stabilization Factors in Crowded Polymer Solutions by Forming Self-Assembled Monolayers on Gold Nanoparticles. *Langmuir* **2013**, *29*, 6018−6024.
(55) Wuelfing, W. P.; Gross, S. M.; Miles, D. T.; Murray, R. W. Nanometer Gold Clusters Protected by Surface-Bound Monolayers of Thiolated Poly(Ethylene Glycol) Polymer Electrolyte. *J. Am. Chem. Soc.* **1998**, *120*, 12696−12697.
(56) Zhang, X.; Servos, M. R.; Liu, J. Ultrahigh Nanoparticle Stability against Salt, pH, and Solvent with Retained Surface Accessibility via Depletion Stabilization. *J. Am. Chem. Soc.* **2012**, *134*, 9910−9913.
(57) Zheng, M.; Davidson, F.; Huang, X. Ethylene Glycol Monolayer Protected Nanoparticles for Eliminating Nonspecific Binding with Biological Molecules. *J. Am. Chem. Soc.* **2003**, *125*, 7790−7791.
(58) Latham, A. H.; Williams, M. E. Versatile Routes toward Functional, Water-Soluble Nanoparticles via Trifluoroethylester-PEG-Thiol Ligands. *Langmuir* **2006**, *22*, 4319−4326.
(59) Barr, T. L.; Seal, S. Nature of the Use of Adventitious Carbon as a Binding Energy Standard. *J. Vac. Sci. Technol. A* **1995**, *13*, 1239−1246.